Title: Performance improvements to MSF plants using forward osmosis

Authors: Peter Nicoll[1], Dario Breschi[2], Brian Moore[1], Tzeyen Chiu[1], Mufeed Hassan[1]

1 – Modern Water plc

2 – Bilfinger Deutsche Babcock Emirates LLC

Abstract

Forward osmosis based processes have shown much promise but have struggled to gain mainstream market acceptance, despite some of their key characteristics, such as low membrane fouling propensity. There are increasing demands for improving the energy efficiency of thermal desalination plants, however these are severely limited and generally are associated with increasing the number of stages or increasing the top brine temperature (TBT).

Modern Water has a patented process that has not been utilised before, which is to couple the multi stage flash desalination process with forward osmosis. In this particular case a portion of the blowdown stream is osmotically diluted by the cooling water and then reintroduced to the recirculating brine. This has the effect of changing the composition of the brine, so that for instance alkalinity and hardness levels are reduced with a reduction in scaling potential. This opens up the opportunity to increase the top brine temperature with all the corresponding advantages, such as lower steam consumption and/or increased output. This presents the possibility of a practical method for increasing performance and/or output via a relatively simple retrofit compared to physically increasing the number of stages.

This paper presents some of the result of a study aimed at evaluating the potential benefits achievable in real cases from the retrofitting of MSF units by FO brine dilution. Two interacting models (chemical and thermodynamic) of the process have been built and various configurations of the coupled (hybrid) plant have been simulated to seek to determine the most effective solution. The configuration with increased top brine temperature and reduced brine recirculation flow appears to be the one bringing the most significant advantages. At a TBT of 131°C, 12% less steam and 27% less power consumption was achieved compared to the design condition.

MSF plants in almost all real cases are coupled to a power cycle supplying low pressure steam at a theoretical marginal cost. The assessment of the benefits (mainly in terms of fuel saving) of the coupled process have been evaluated for a typical power-desalination plant located in the GCC region, taking into account the actual operating constraints dictated by the seasonal variations in power and water demand. This modelling indicated that an 8% decrease in fuel consumption could be achieved for the hybrid plant. The capital and operating costs for the FO plant were evaluated, giving an indicative payback period in the range of 18 months to five years depending on the dual-purpose plant configuration, site constraints and fuel purchase by the plant owner/operator.

1 Introduction

Forward osmosis based processes have shown much promise but have struggled to gain mainstream market acceptance, despite some of their key characteristics, such as low membrane fouling propensity and in certain processes, low energy consumption compared to competing processes. There are increasing demands for improving the energy efficiency of thermal desalination plants, however these are severely limited and generally are associated with increasing the number of stages or increasing the top brine temperature (TBT).

Modern Water has a patented process, for instance EP2498135 and US9156712, which has not been exploited before, which is to partially couple the multi stage flash desalination process (or indeed any thermal process) with forward osmosis. In this particular case a portion of the blowdown stream is osmotically diluted by the cooling water and then reintroduced to the recirculating brine. This has the effect of changing the composition of the brine, so that for instance alkalinity and hardness levels are reduced with a reduction in scaling potential. This opens up the opportunity to increase the top brine temperature with all the corresponding advantages, such as lower steam consumption and/or increased output. This presents the possibility of a practical method for increasing performance and/or output via a relatively simple retrofit compared to physically increasing the number of stages as discussed by Al-Najdi et al. (2015).

The approach taken to assess the process, was to develop models for both the chemistry and thermodynamic/design of the combined MSF and FO processes. This then allowed the impact of the coupling of the two processes to be assessed.

This paper outlines the methodology used for developing the chemistry model of the combined processes and its coupling with a model for the MSF process. A typical MSF plant operating at a design TBT of 108°C is coupled with FO and the TBT is increased by maintaining the same scaling potential as the original design condition, by the use of osmotic permeate addition to the recirculating brine.

2 MSF-FO Integration

The MSF system can be categorised into the three sections indicated in Figure 1; brine heater, heat recovery section and heat rejection section. The feed to the brine heater flows through the tubes of the heat recovery section stages where its temperature increases until it reaches the inlet of the brine heater. It is heated by the condensation of the vapour flashed off in each stage. Low pressure steam is used to provide the heat input to elevate the brine to its top brine temperature (TBT).

The heated brine then passes into the first stage of the heat recovery section where low pressure is maintained and vapour flashes off. The vapour condenses as distillate on the tubes, and the distillate produced passes to the subsequent stage until it is extracted at the last stage of the heat rejection section. Similarly, the residual brine passes from stage to stage and becoming progressively more concentrated until it reaches its maximum concentration in the final stage of the heat rejection section. The recirculating brine is combined with make-up seawater which is pre-treated (deaerated and dosed with antiscalant, antifoam and oxygen scavenger) before being pumped back as feed to the last heat recovery stage. The brine blowdown is drawn from the final stage of the heat recovery section. A portion of the brine blowdown from the last stage of the heat rejection section is used as the (high osmotic pressure) draw solution to the forward osmosis (FO) membranes. Heated seawater from the heat rejection section is used as the feed solution to the FO membranes. The FO

membranes are selectively permeable and osmosis causes permeate to pass from the feed solution side to the draw solution side of the membranes, thus diluting the draw solution (brine). This diluted brine from the FO system is along with the combined recirculating brine and seawater make-up stream are then recycled back as feed to the heat recovery section. The net effect, being a dilution of the brine entering the brine heater. The high rejection of the FO membranes also results in a portion of the high molecular weight additives from the brine blowdown used as FO draw solution being retained and recycled.

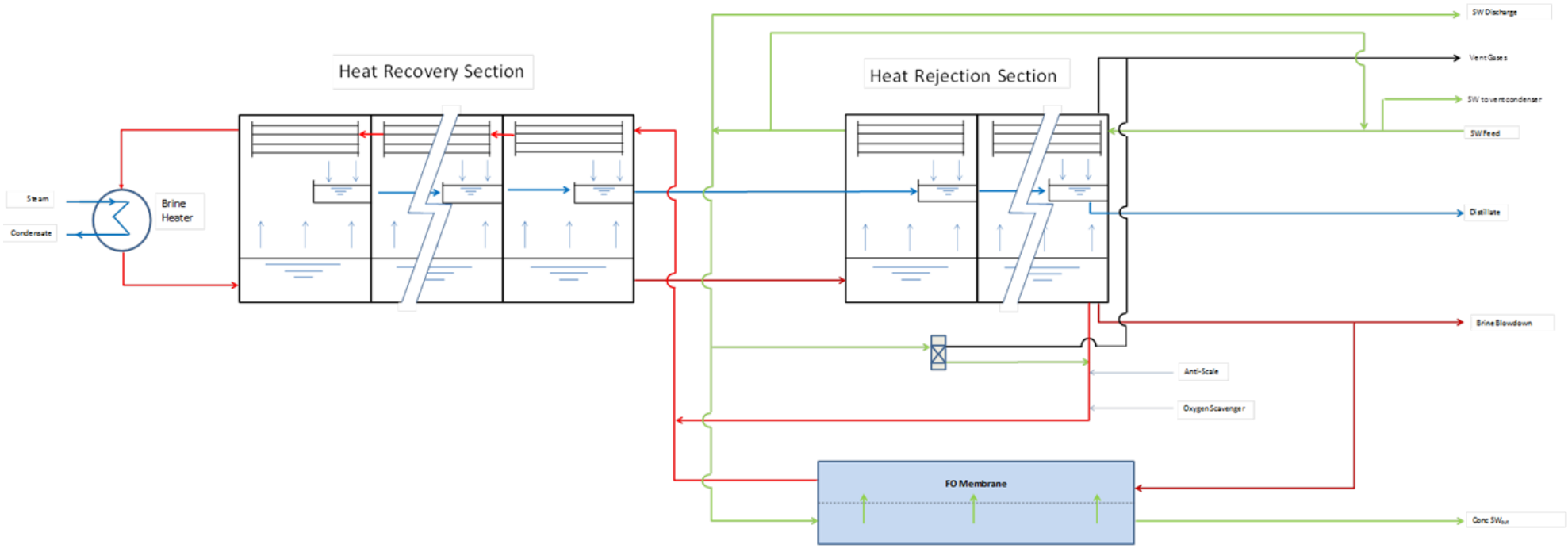

Figure 1: Process Schematic of the MSF FO Plant

3 Modelling of the process

3.1 Chemical Model

A chemical model has been developed to determine the mass flow and composition of the fluid in all streams of the combined MSF and FO processes. The model is run within a spreadsheet using Visual Basic for Applications (VBA) code. This model has been used to predict the changes in composition, and therefore the risk of scaling of sparingly soluble salts for each process stream, whilst simulating changes to the process such as changing the TBT, the brine recycle flow or the permeate flow through the FO membranes.

The FO system in this paper has been modelled for simplicity to assume both divalent and monovalent ions are 100% rejected, which is a valid starting approximation. Additionally, the FO recovery has been set to 20%, in can of course be varied. In order to specify the performance of the FO membranes, a target of 1 g/kg concentration difference between the dilute draw solution and the feed solution has been set. FO membrane projections were subsequently performed to establish the membrane area required to achieve this level of performance. This is an area for further optimisation relating to both capital and operating costs, which may be the subject of a future paper.

Within the model, at each process node an overall mass balance is performed as well as a mass balance for individual ions, thus allowing the composition of each stream to be determined.

3.2 Derivation of the Physicochemical Characteristics of the streams

The temperature, pressure and mass flow of all the relevant streams except those streams associated with the FO system are based on the relevant data from a reference MSF unit. The temperature and pressures of the FO system streams have been derived assuming that heat and pressure losses are minimal.

The salinity (S) of the inlet seawater has also been taken from the reference MSF unit based in one of the GCC countries. The ionic composition of the seawater feed is derived from its salinity, using the ratio of individual ions in standard seawater for all ions with the exception of the inorganic carbon compounds. The inorganic carbon compounds namely carbon dioxide (CO_2), bicarbonates (HCO_3^-) and carbonates (CO_3^{2-}) are pH, salinity and temperature dependant thus using a standard seawater composition can introduce errors to these calculations. The derivation of the concentrations of these compounds is described in Section 3.2.1.

3.2.1 Carbonate System

The model solves the chemical equilibria of the carbon dioxide, bicarbonate and carbonate system using data presented by Millero (1995) based on the experimental data of Goyet and Poisson (1989) and Roy et al (1993), which define correlations for the system dissociation constants as a function of temperature and salinity. Thus, the pH of each stream (except the feed stream which is based on the pH data for the reference MSF unit) is also determined within the model using the equations contained in Appendix A:

$$H_2O \xleftrightarrow{K_w} H^+ + OH^- \quad \textbf{(1)}$$

$$CO_2(g) \xleftrightarrow{K_0} CO_2(aq) \quad \textbf{(2)}$$

$$CO_2 + H_2O \xleftrightarrow{K_1} H^+ + HCO_3^- \quad \textbf{(3)}$$

$$HCO_3^- \xleftrightarrow{K_2} H^+ + CO_3^{2-} \quad \textbf{(4)}$$

where K_w is the dissociation constant for water:

$$K_w = [H^+][OH^-] \quad \textbf{(5)}$$

K_0 is the solubility coefficient of carbon dioxide in seawater and K_1 and K_2 are the dissociations constants for carbonic acids respectively:

$$K_1 = \frac{[H^+][HCO_3^-]}{[CO_2]} \qquad K_2 = \frac{[H^+][CO_3^{2-}]}{[HCO_3^-]} \quad \textbf{(6)}$$

The concentrations of carbon dioxide, bicarbonate and carbonate in the feed water are calculated based on the seawater pH (user-defined) and the correlations between total alkalinity (TA), chlorinity (Cl) and salinity (S) from Millero (1996):

$$TA = 0.0001185\,Cl \quad \textbf{(7)}$$

Where $Cl = \frac{S}{1.80655}$

The relationship between carbonate alkalinity (CA) and TA is

$$\mathrm{CA} = \mathrm{TA} - [\mathrm{B(OH)_4^-}] + [\mathrm{H^+}] - [\mathrm{OH^-}] \quad \textbf{(8)}$$

where $[B(OH)_4^-]$ is the concentration of tetrahydroxyborate and $\mathrm{CA} = [\mathrm{HCO_3^-}] + 2[\mathrm{CO_3^{2-}}]$

The higher temperatures around the brine heater impact the carbonate equilibria and thus influence the risk of scaling. Since the streams are considered a closed system ahead of the first stage of the MSF plant, the carbon dioxide is all treated as aqueous thus the total inorganic carbon (TIC) remains the same. With the additional calculation of the first and second dissociation constants, the relative concentrations can be given in terms of total inorganic carbon content:

$$[HCO_3^-] = \frac{[H^+]K_1}{[H^+]^2 + [H^+]K_1 + K_1K_2}\,TIC \quad \textbf{(9)}$$

where:

HCO_3^-, H^+ = concentration of bicarbonate and hydrogen in mol/l respectively

K_1, K_2 = first and second dissociation constants of carbonic acid

TIC = total inorganic carbon in mol/l $[CO_2] + [H_2CO_3] + [HCO_3^-] + [CO_3^{2-}]$

$$[H_2CO_3] = [CO_2aq] = \frac{[H^+]^2}{[H^+]^2 + [H^+]K_1 + K_1K_2}\,TIC \quad \textbf{(10)}$$

where:

H_2CO_3 (CO_2aq), H^+ = concentration of aqueous carbon dioxide and hydrogen in mol/l respectively

K_1, K_2 = first and second dissociation constants of carbonic acid

TIC = total inorganic carbon in mol/l $[CO_2]+[H_2CO_3]+[HCO_3^-]+[CO_3^{2-}]$

$$[CO_3^{2-}]=\frac{K_1K_2}{[H^+]^2+[H^+]K_1+K_1K_2}TIC \quad \textbf{(11)}$$

where:

CO_3^{2-}, H^+ = concentration of carbonate and hydrogen in mol/l respectively

K_1, K_2 = first and second dissociation constants of carbonic acid

TIC = total inorganic carbon in mol/l $[CO_2]+[H_2CO_3]+[HCO_3^-]+[CO_3^{2-}]$

The concentration of H^+ ions is calculated using the dissociation constant of water (equation 5). Since an increase in K_W allows for higher dissociation of H_2O into H^+ and OH^-, the concentration of H^+ ions can be calculated using the predicted change in K_W for higher temperature streams.

$$[H^+]_{21/22}=\frac{K_{W\,21/22}}{K_{W\,20}}[H^+]_{20} \quad \textbf{(12)}$$

The majority of the process nodes simulate the blending or splitting of streams where the determination of the mass flow and composition of resultant streams is straightforward. However, in some instances chemical reactions or phase changes occur and the approaches used in these cases are described here in more detail.

The loss of dissolved carbon dioxide from the seawater make-up stream to the vapour phase in the deaerator is modelled by defining a carbon dioxide removal efficiency for the deaerator. The removed carbon dioxide is then vented out of the system.

The extent of thermal decomposition of bicarbonate within the flash distillation chambers is evaluated based on the findings reported by Genthner et al, (1993) who studied non-condensable gases in sea water distillers, observing that the decomposition of bicarbonate is not completed when the brine leaves the plant. The authors observed that up to two thirds of the bicarbonates from the make-up water thermally decompose. The model therefore permits the user to define the proportion of make-up water bicarbonate decomposed in the distillation process. The masses of carbonates and carbon dioxide generated by the thermal decomposition of bicarbonate are calculated on a molar basis in accordance with equation 13 below:

$$2HCO_3^- \leftrightarrow CO_3^{2-}+CO_2+H_2O \quad \textbf{(13)}$$

3.2.2 Scaling

Scaling of the MSF internal surfaces may occur when sparingly soluble salts are concentrated within the process beyond their solubility limit.

In MSF distillers the most commonly observed scales that occur are found to be calcium carbonate ($CaCO_3$), magnesium hydroxide ($Mg(OH)_2$) and less commonly calcium sulphate ($CaSO_4$). Other common sparingly soluble salts encountered in desalination processes are calcium sulphate ($CaSO_4$),

calcium carbonate ($CaCO_3$), calcium fluoride (CaF_2), barium sulphate ($BaSO_4$), strontium sulphate ($SrSO_4$) and silica (SiO_2).

For each of the sparingly soluble salts, the saturation index (SI) has been calculated, which is defined as the logarithm of the ratio of the ionic product (IP) and the solubility product (K_{sp}), $SI = \log_{10}(IP/K_{sp})$. The ionic product is calculated as the product of the ionic concentrations of the relevant ions. The solubility product for any salt varies with pressure, temperature, ionic strength and pH. Therefore, a saturated solution will have a SI of 0, an undersaturated solution will have a negative SI, and a supersaturated solution will have a positive SI. A positive SI is only an indicator that scale formation is possible as scale formation is complex and depends upon kinetics and the presence of nucleation sites for crystal formation. The sections below describe the methodology used to evaluate the SI of each sparingly soluble salt, and the detailed correlations employed can be found in Appendix B.

3.2.2.1 Derivation of Calcium Carbonate Saturation Index

The derivation of $CaCO_3$ scaling potentials follows the Oddo-Tomson method which is commonly used in the oil industry. It is valid between 0 - 200°C, ionic strengths of 0 - 4 and pressure of 1-1380 bar. Other methods, such as the Langelier saturation index (LSI) Stiff and Davis Stability Index (S&DSI), also predict calcium carbonate scaling tendencies. However, they both have built-in constraints in that neither accounts for the influence of pressure and temperature on the solubility of CO_2.

The correlation described in Oddo et al (1998) calculates the saturation index for $CaCO_3$ with gas phase being absent. Since each stream is essentially a closed system with nowhere for the gas to escape, the CO_2 is assumed to be in aqueous form.

3.2.2.2 Derivation of Magnesium Hydroxide Saturation Index

The derivation of magnesium hydroxide follows a study done by Carlson et al (1953) who investigated the solubility of $Mg(OH)_2$ at different temperatures in the range of 30°C to 250°C. The correlation describes the calculation of the solubility product which is then used to calculate the SI.

3.2.2.3 Derivation of Calcium Sulphate Saturation Index

Oddo et al (1998) also describes the SI for calcium sulphate. Under the temperature conditions observed in MSF plants, there exists two phases of calcium sulphate. Gypsum is the most common scale former and occurs at temperatures below 90°C whilst anhydrite becomes the stable form of calcium sulphate above 90°C. The anhydrite form therefore becomes relevant when assessing the likelihood of scaling around the brine heater.

3.2.2.4 Derivation of Barium Sulphate Saturation Index

The solubility product for barium sulphate follows the method found in ASTM D4328-03 which is valid from 25°C to 95°C. Oddo et al (1998) can also be used to calculate the SI and is valid up to 200°C. The saturation index results predicted using the two methods described are fairly consistent (10-20% difference) at temperatures below 95°C. Either one can be used for temperatures up to 95°C but above this the Oddo-Tomson method should be used, as in our model.

3.2.2.5 Derivation of Strontium Sulphate Saturation Index

The scaling potential of strontium sulphate can be derived by two methods. ASTM D4328-03 calculates the $K_{spSrSO4}$ at various ionic strengths over a temperature range of 38-149°C and pressures up to 3000 psig derived from experimental $SrSO_4$ solubility data obtained from McDonald et al

(1969). Additionally, the Oddo-Tomson method (1998) allows the strontium sulphate or celestite saturation index to be calculated. Comparison of both methods show that the results to be fairly consistent (10-20% difference). Either method can be used for temperatures up to 149°C, our model uses the Oddo-Tomson approach.

3.2.2.6 Derivation of Calcium Fluoride Scaling Potentials

The derivation of calcium fluoride uses the Du Pont (1983) method to predict the solubility product at 25°C. This method, however, does not account for temperature and it is known that CaF_2 solubility increases then decreases with increasing temperature. The Van't Hoff method has been used to correct for different temperatures following the approach taken by Wolfe et al (2000).

3.2.2.7 Derivation of Silicon Dioxide Scaling Potentials

The scaling potential of soluble silica (silicic acid) has been calculated following ASTM D4993-89 (Reapproved 2003) which is valid up to 45°C. The solubility of SiO_2 is read off the solubility of SiO_2 vs. temperature graph and corrected for pH by multiplying the solubility by the pH correction factor obtained from the SiO_2 pH correction factor.

3.3 Thermal Model

A thermodynamic model of a conventional MSF plant is used to simulate the plant performance in off -design conditions. The model performs the overall heat and mass balance of the system and the detailed calculation of the physical parameters in each stage of the plant. Thus the thermodynamic model evaluates the brine heater low pressure (LP) steam conditions and mass flow rate, and the gained output ratio (GOR) for varying flow and TBT conditions. The influence of non-equilibrium losses, boiling point elevation, fouling factors and vapour head losses are calculated for each stage by empirical correlations. The thermodynamic model allows the estimation of the electrical power absorbed by the MSF plant auxiliaries at the selected operating conditions.

4 Scope of Modelling

The models have been used to predict the performance of the integrated MSF and FO processes across a range of flow and thermal conditions. The scope of the modelling was twofold; to investigate how a) distillate output capacity and b) the energy efficiency of existing MSF plants could be improved by the incorporation of FO permeate dilution of the brine.

The thermal and chemical models were first run for the reference MSF plant to establish a set of base case conditions. In both investigations, the approach taken was to adjust the degree of brine dilution such that the scaling potential at the exit of the brine heater was maintained the same as for the base case, whilst increasing the TBT. The scaling potential was evaluated based on the $CaCO_3$ scaling index as this was deemed to present the greatest risk of scaling at higher temperatures because $CaCO_3$ solubility decreases with increasing temperature.

The thermodynamic and chemical models were not directly linked. The two models were run separately and iteratively to match the thermal and mass balance conditions from the thermodynamic model with the predicted stream compositions from the chemical model.

A number of considerations and constraints were included to ensure the practical feasibility of the revised conditions:

- Diluted brine TDS had to be greater than the seawater TDS.
- Concentrated seawater TDS not exceeding that of the brine.
- Maximum allowable vapour velocity through the demisters
- Maximum power absorbed by the installed pumps
- Maximum attainable steam condensation pressure in the brine heater

a) Increasing Distillate Output

The potential for using FO to increase the distillate production of existing MSF facilities was evaluated. The approach taken was to model the MSF operation at increasing TBT, whilst maintaining the same scaling potential for $CaCO_3$ as the MSF base case at the exit of the brine heater, by increasing the degree of brine dilution with FO permeate. The increased TBT results in an increase in distillate production as the flash range is extended and the evaporation rate in each stage is increased. Two constraints were imposed to limit the requirements to modify an existing MSF plant to accommodate the revised hydraulic conditions; the total brine flow to the heat recovery section was maintained equal to the MSF base case, and the same seawater make-up flow as the MSF base case was also assumed.

b) Increasing Energy Efficiency

The potential for using FO to increase the energy efficiency of existing MSF facilities was evaluated. Here the distillate output has been fixed relative to the base case, whilst the TBT has been increased by diluting the recycled brine to maintain the same $CaCO_3$ scaling potential as the MSF base case at the exit of the brine heater. The rationale here was by increasing the flash range and keeping the distillate flow rate constant, the brine recirculation flow rate can be reduced hence allowing a decrease in specific energy consumption. The energy efficiency was measured using the performance ratio (PR) and gained output ratio (GOR). Again, the seawater make-up flow has been fixed as equal to that for the base case to limit the requirements to modify an existing MSF plant.

5 Simulation of FO-enhanced MSF plant operation

5.1 Object and aim of the simulation

The chemical and thermodynamic models described in the previous sections have been used to perform an extensive simulation of the operation of a reference MSF plant upgraded with FO-diluted seawater make-up system. The aim of the simulation runs was to establish the most effective way to enhance the performance of the distiller taking advantage from the reduced scaling potential.

The reference MSF unit considered in our study is typical of the installed fleet in the Gulf Cooperation Countries (GCC), its main features being summarised in Table 1. The FO-enhanced configuration of the distiller is the one depicted in Figure 1. Part of the brine discharged from the MSF unit is conveyed as draw solution to the Forward Osmosis membranes, is diluted by a stream of seawater from the Reject Section condensers and is finally mixed with the main stream of recirculated brine.

Distillate production	12	MIGD
Performance Ratio	8.7	kg / 2326 kJ
Top Brine Temperature	108	°C
Flash Range	69.4	°C
Number of stages	20	

Table 1 - Design parameters of the reference MSF unit

The simulation cases have been calculated by iterating between the chemical and thermodynamic models. We have considered in our calculations progressively higher values for the top brine temperature of the MSF unit, while in parallel increasing the dilution of the brine stream recycled through the FO membranes. The criteria for adjusting these operating parameters was to maintain in all simulation cases a sensibly constant value of the critical Solubility Indexes in the high-temperature sections of the MSF distiller, thus avoiding any increase in the scaling potential of the brine. Due to the unaltered values of SI's in the upgraded conditions, all cases have been calculated considering in the thermodynamic model the same Fouling Factors as in the reference (design) operating conditions of the MSF plant.

In order to identify the operating parameters of the distiller with the integrated FO system, two series of simulation cases were carried out:

a) Operation of the MSF distiller at increased TBT and constant brine recirculation flow rate, leading to increased distillate production;

b) Operation of the MSF distiller at increased TBT and reduced brine recirculation flow rate, in order to keep a constant distillate production.

5.2 Increase in distillate production

The main results of the simulation runs related to the operation of the reference MSF plant at increasing TBT and constant brine recirculation flow rate are summarised in Figure 5-1 and Figure 5-2.

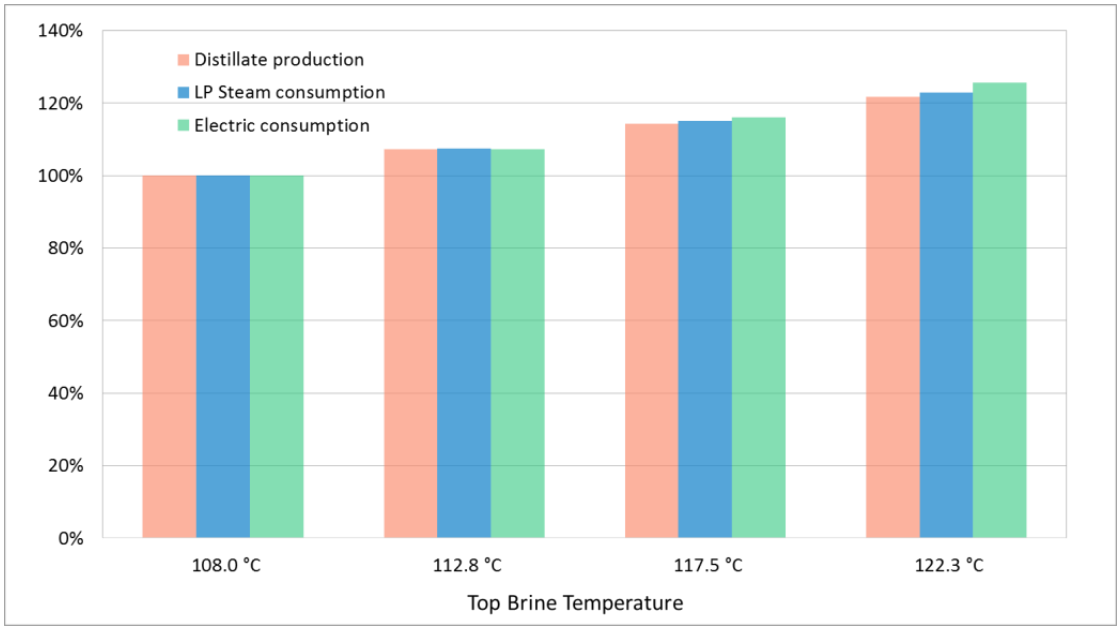

Figure 5-1 - Operation of the MSF-FO unit at increasing distillate production

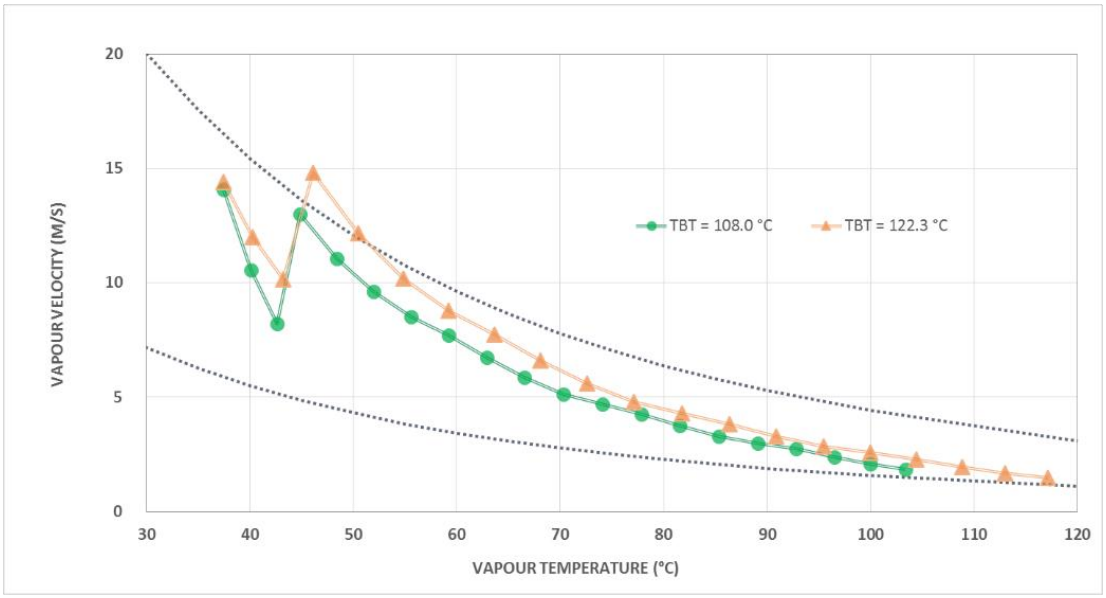

Figure 5-2 - Vapour velocity through demisters at increasing production

Our analysis of the calculation results brings to the following considerations.

- Figure 5-1: Our simulation shows that with a constant brine recirculation flow rate and increasing the top brine temperature, the distillate production of the modelled MSF plant increases linearly with the flash range, inline with theory. Also not surprisingly, the steam consumption increases almost linearly with the production, whilst the electrical consumption rises more sharply (mainly due to the non-linearity of head losses).
- Figure 5-2: The calculation of the vapour flow through the demisters in the selected operation cases shows that, due to the geometrical sizing of the reference evaporator, the limit velocity is exceed in a couple of stages at the 122.3°C operating case.
- In order to cope with the rise in flow rates (notably brine recirculation and cooling seawater) required by these operational cases, some upgrade in the installed centrifugal pumps (impeller / driver) has to be considered.

In view of the practical limitations in raising the production capacity in existing MSF units, it has not been deemed worthwhile to extend the investigation to cases with higher values of TBT.

5.3 Efficiency improvement

The second series of simulation runs has been carried out considering an increase in TBT (in steps from the design value of 108°C up to 131°C and a corresponding decrease in the brine recirculation flow rate through the reference MSF unit, in such a way as to keep (by iterative calculation) a constant distillate production in all cases. The main results of these simulation runs are summarised in Figure 5-1 and Figure 5-2.

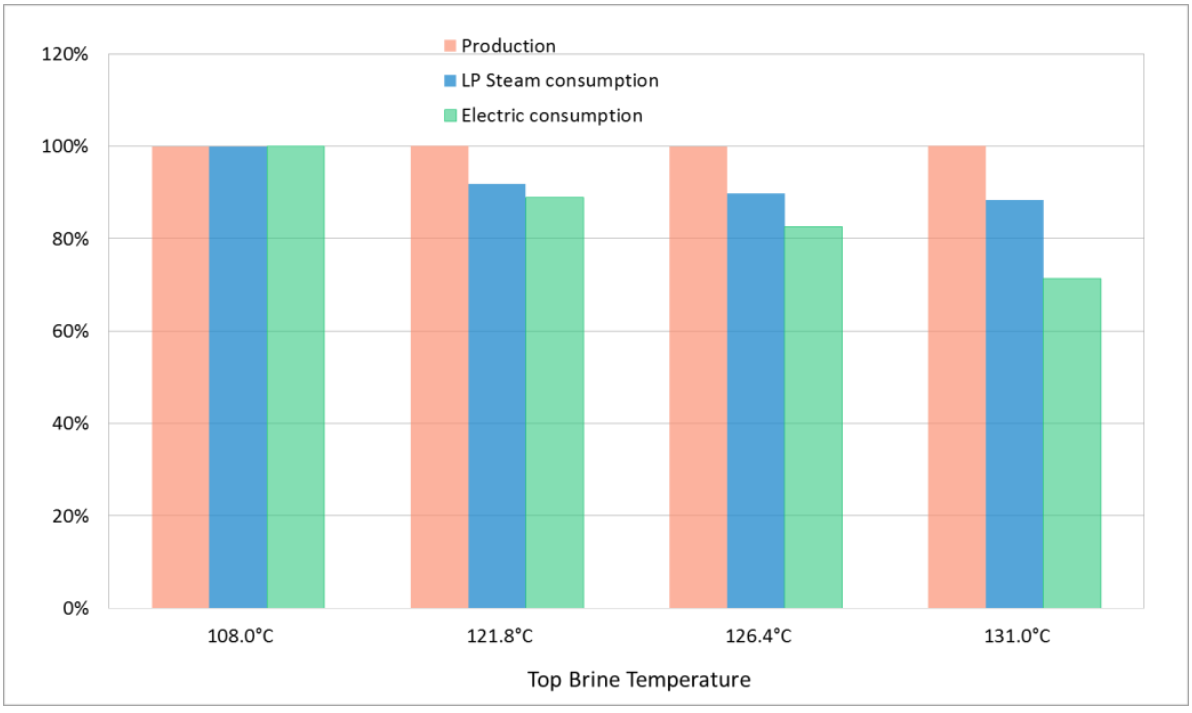

Figure 5-3 - Operation of the MSF-FO unit at improved efficiency

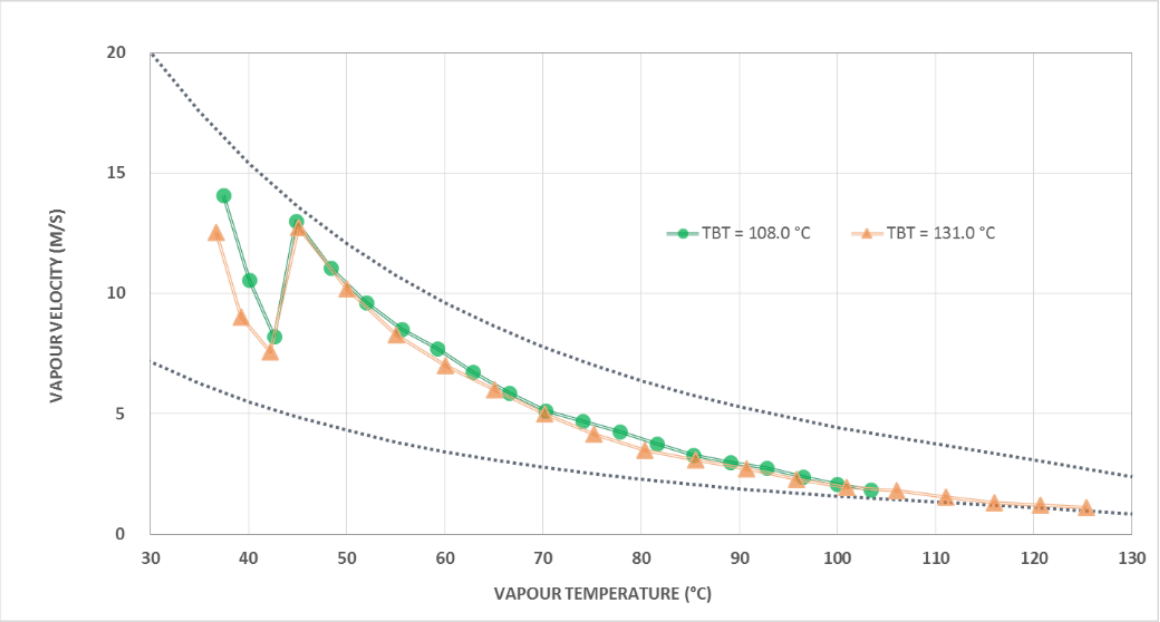

Figure 5-4 - Vapour velocity through demisters at improved efficiency

Main observations:

- Figure 5-3: Increasing the flash range whilst reducing the brine recirculation flow rate in the MSF distiller allows decreasing the specific energy consumption of the distiller, both thermal and electrical. The thermal efficiency improvement is explained by the fact that the wider flash range allows a larger heat recovery inside the evaporator, thus reducing the requirement for external heat input (steam to the brine heater). The reduction in electrical absorbed power is related to the lower flow / head required by the main centrifugal pumps (brine recirculation and cooling seawater supply) in the upgraded condition.

  The savings in steam and auxiliary power consumption are evaluated respectively at 12% and 27% for the upgraded distiller operation at 131°C TBT, as compared to the original design operating conditions.

- Figure 5-4: The calculation of the vapour flow through demisters in the selected operation cases shows that the values of vapour velocity are well within the allowed range.

- No major modification to the MSF plant equipment is necessary to allow proper operation at all the above operating conditions. The higher differential pressure and lower brine flow rate across the evaporator stages may be accommodated by a simple reduction in the area of the inter-stage brine orifices.

5.4 FO Integration

Analysing both scenarios, it can be concluded that improving the energy efficiency of the plant is more viable. It minimises any modifications made to that plant if scenario A was chosen i.e. having to select larger demisters and a larger distillate pump.

It was found that increasing the GOR of the plant satisfied both chemical and thermal constraints as described previously. A 10% increase in GOR outweighs the increase in distillate seen in the other scenario, however this may not be the case for new build plant designed to exploit the increased output. This may be presented in a future paper.

6 Analysis of FO-enhancement benefits in a reference cogeneration scheme

It appears from the analysis carried out in the previous section that the main benefits of the proposed FO upgrade of operating MSF plants is reducing the specific energy consumption for water production (up to 12% and 27% respectively for steam and electricity in the limited cases we examined). In order to properly assess the actual economic value of such an improvement, it is necessary to translate these figures in terms of associated fuel saving. Since almost all installed MSF units worldwide are coupled to the steam cycle of a power plant, it is necessary to define in advance the reference cogeneration process integrating the MSF plant and the related operation modes in order to properly assess the related fuel consumption.

6.1 Reference cogeneration scheme

Figure 6-1 - Reference cogeneration plant scheme depicts the flow diagram of the dual-purpose plant considered in our exercise. It consists of three gas turbines with associated heat recovery steam generator's (HRSG's) at single pressure level with duct firing and one back-pressure turbine discharging low pressure (LP) steam to four MSF distillers. A similar arrangement of the plant modules may be found in most independent water and power producers (IWPPs) in the GCC countries.

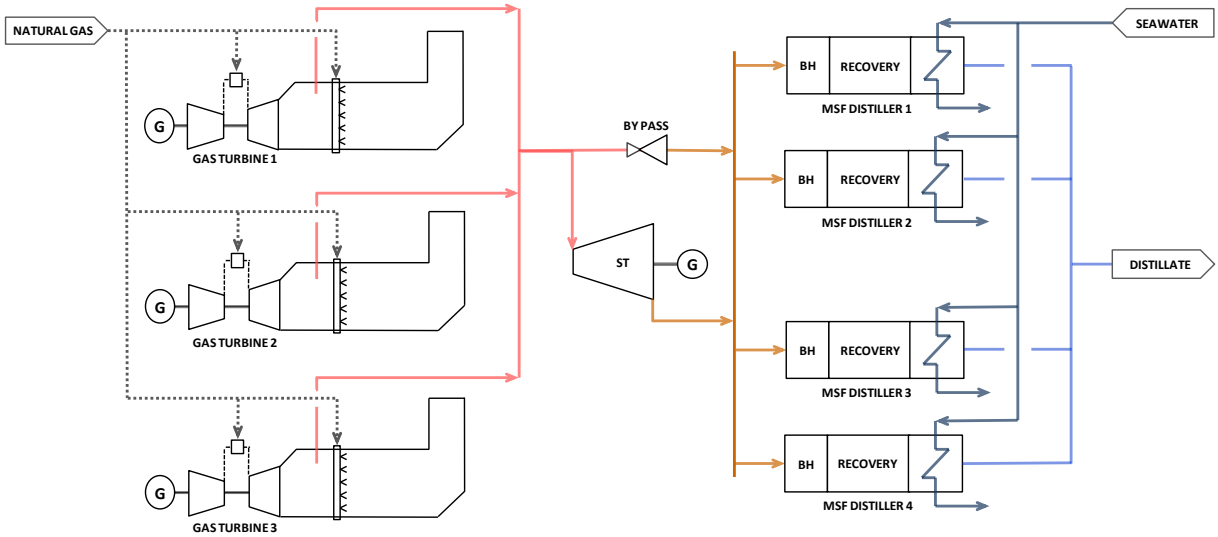

Figure 6-1 - Reference cogeneration plant scheme

The design data of the cogeneration plant assumed in our assessment, is typical of the installed fleet in the region, are the following:

- Power Production Capacity
  - *3 x 123 MW Gas Turbines*
  - *1 x 220 MW Back pressure Steam Turbine*
- HRSG steam generation: *295 kg/s at 79 bar and 565°C*
- Water Production
  - *4 x 12 MIGD MSF Distillers*
- Total Power Production Capacity: 585 MW
- Total Water Production Capacity: 48 MIGD

6.2 Reference operational modes of the cogeneration plant

Figure 6-2 (taken from Kennedy et al. (2012)) shows the typical seasonal variation of power and water demand in the GCC countries. It can be observed that, while the water consumption is fairly constant along the year, the power requirement has a peak in summer months (the main reason being the high consumption of air conditioning equipment) and sharply decreases for the rest of the year, falling below 40% in the winter season. As a consequence of this load profile, during most of the operating period the boiler has to generate steam in excess of the requirement for power production, in order to provide to the distillers the heat input necessary to meet the water demand. Therefore frequently cogeneration plants like the one shown in Figure 6-1 are operated with supplementary firing on and the steam turbine by-passed. This operational constraint implies a considerable increase in the overall fuel consumption throughout the year as compared to the design condition, which has to fully considered when evaluating the benefits in improving the efficiency of the distiller.

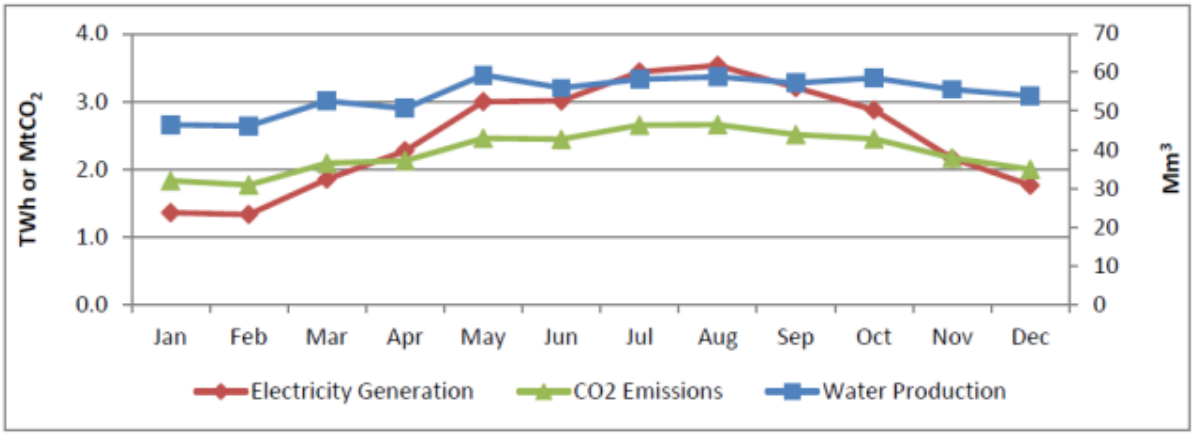

Figure 6-2 - Seasonal variations of 2008 electricity-water demand and CO_2 emissions in the Gulf

6.3 Evaluation of fuel savings

A simplified model of the cogeneration plant depicted in Figure 6-1 has been used in order to evaluate the effect of the improved performance of the FO-retrofitted MSF plant, on the overall fuel consumption for power-water production. We have considered in our evaluation a value of 131°C for the top brine temperature of the MSF plant (see section 5.3) and plant load at 40% and 80% of the design capacity for power and water production respectively (see section 6.2).

In the selected operational mode of the cogeneration plant, the gas turbines are run at part load, the duct firing level is set for producing in the HSRG the amount of steam required by the distillers and the steam turbine is partially by-passed in order to match the power demand from the grid.

The operating parameters of the dual-purpose plant, both in the conventional configuration and in the FO-retrofitted one, are presented in Figure 6-3. The improvement in MSF distillers efficiency (i.e., increase in Performance Ratio) and the decrease of auxiliary electrical consumption allows reducing the level of duct firing necessary for generating the amount of steam required for water production, with a consequent overall fuel saving evaluated at 8% in the analysed case.

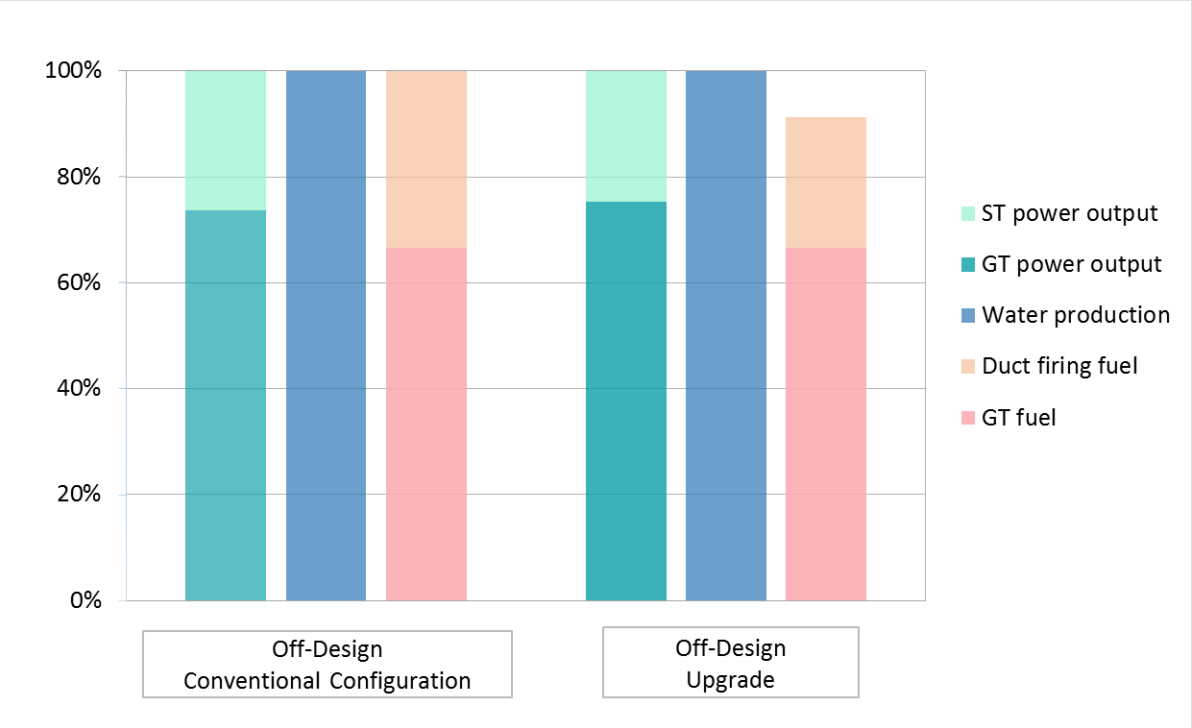

Figure 6-3 - Operation parameters of the dual-purpose plant

6.4 Economic considerations

In order to assess the cost-effectiveness of the proposed solution, we have carried out an overall estimation of the payback period for the FO-retrofitting of the MSF plant. To this aim, we have evaluated the following cost elements, consistently with the assumptions mentioned in the previous sections:

- Investment cost for the installation of the new equipment in existing site (FO membranes and related pre-treatment sections);
- Additional O&M cost for the FO system;
- Saving in fuel consumption, according to the calculation outlined at Section 6.3.

For each of the above cost figures we have determined a sensible range of variation, depending on the specific dual-purpose plant configuration, on the actual site constraints and on the existing

conditions for fuel purchase by the plant owner / operator. Considering these variations, the payback period for the retrofitting varies between 18 months and five years.

7 Conclusions

The integration of FO and the multi stage flash desalination process as outlined in European patent EP2498135 etc has been modelled both chemically and thermodynamically. This combined modelling shows that an osmotic dilution of the recirculating brine using the seawater cooling water lowers the scaling propensity. Consequently the TBT may be increased while still maintaining the same scaling indices as a plant configured without the enhancement, thus allowing an increase in distillate from the plant or a reduction in energy consumption – both steam and electrical. It is this later condition that appears to be the most attractive in terms of existing MSF plants, given both the value of the energy saved and the minimal changes to the MSF plant and equipment.

Alternative methods of improving MSF plant efficiencies such as physically increasing the number of stages would require significant downtime of the asset. This approach of partially coupling MSF with FO is much simpler and would not require the same disruption to production because the MSF plant could continue to operate while the FO system was being built.

The economic assessment of coupling the two processes is complex given MSF plants are normally integrated with a combined cycle power station, with significant electrical load variations throughout the year but little change in water demand. In one representative configuration, located within the GCC, the coupling of the processes leads to an 8% reduction in fuel consumption of the combined cycle power plant. The payback period is clearly project specific, depending on the cost of fuel and the plant configuration, but was estimated to be within the range of 18 months to five years. Further work is being done to develop the economics of the process, which we anticipate will make the process even more attractive.

References

Peter Nicoll, Thermal Desalination, European Patent EP2498135, 2013

Peter Nicoll, Thermal Desalination, US Patent US9156712, 2015

Othman Y. Al-Najdi, Osman A. Hamed, Khalid H. Bamardouf, Hiroshi Sadayuki, Yoshiyuki Hatano, An innovative approach to reduce energy consumption of SWCC's existing MSF plants, Proceedings IDA World Congress, San Diego, USA, August/September 2015

John. E. Oddo and Mason. B. Tomson, Methods predicts well bore scale, corrosion, Oil and Gas Journal, 96, 23, 1998

ASTM D3739-05, Standard Practice for Calculation and Adjustment of the Langelier Saturation Index for Reverse Osmosis, ASTM International, West Conshohocken, PA, 2005, www.astm.org

ASTM D4582-05, Standard Practice for Calculation and Adjustment of the Stiff and Davis Stability Index for Reverse Osmosis, ASTM International, West Conshohocken, PA, 2005, www.astm.org

ASTM D4328-03, Standard Practice for Calculation of Supersaturation of Barium Sulfate, Strontium Sulfate, and Calcium Sulfate Dihydrate (Gypsum) in Brackish Water, Seawater, and Brines, ASTM International, West Conshohocken, PA, 2003, www.astm.org

C.C. Templeton, Solubility of barium sulfate in sodium chloride solutions from 25° to 95°C, Journal of Chemical & Engineering Data, 5 (1960) 514-516.

J. P. McDonald, Jr., H. L. Skillman and H. A. Stiff, Jr., Paper No. 906-14-I, "A Simple Accurate, Fast Method For Calculating Calcium Sulfate Solubility In Oilfield Brine," presented at the Spring Meeting of the South Western District, API, Lubbock, TX, 1969.

Du Pont Technical Information Manual Volume 1 Section 4, January 1983 (addendum May 1985)

Wolfe, Thomas (2000). "Total flux & Scalant Program: A Membrane System Design Assistant", United States Environmental Protection Agency Project 9C-R193-NTSX.

D.K. Nordstrom and E.A. Jenne, Fluoride solubility equilibria in selected geothermal waters. Geochim. Cosmochim. Acta, 41 (1977) 175-188.

ASTM D4993-89(2003), Standard Practice for Calculation and Adjustment of Silica (SiO_2) Scaling for Reverse Osmosis, ASTM International, West Conshohocken, PA, 2003, www.astm.org

F.J. Millero, Thermodynamics of the carbon dioxide system in the oceans. Geochim. Cosmochim. Acta, 59 (1995) 661-667.

C. Goyet and A. Poisson, New determination of carbonic acid dissociation constants in seawater as a function of temperature and salinity. Deep-Sea Res., 30 (1989) 1635-1654.

R. N. Roy, L.N. Roy, M. Lawson, K.M. Vogel, C. Porter-Moore, W. Davis, F.J. Miller and D.M. Campbell, Determination of the ionization constants of carbonic acid in seawater. Mar. Chem., 44 (1993) 249-268.

F. J. Millero, Chemical Oceanography, 2nd edn., CRC Press, Boca Raton, 1996.

K. Genthner, A. Gregorzewski and A. Seifert, The effects and limitations issued by non-condensable gases in sea water distillers. Desalination, 93 (1993) 207-234

S. Kennedy, S. Sgouridis, P-Y. Lin, A. Khalid, CO2 Allocation for Power and Water Production in Abu Dhabi, Masdar Institute Working Paper, 2012

Appendix A

Saturation Index for $CaCO_3$

$$SI = \log\left(\frac{Ca \times HCO_3^{\,2}}{CO_{2\,aq}}\right) + 3.801 + 8.115\times10^{-3}T + 9.028\times10^{-6}T^2$$
$$- 7.419\times10^{-5}P - 1.961I^{0.5} + 0.695I - 1.136\times10^{-2}I^{1.5} - 1.604\times10^{-4}TI^{0.5}$$

Where:

SI = $\log_{10}(IP/K_{sp})$

IP = Ionic Product = $[Ca^{2+}]$ $[CO_3^{2-}]$ (concentrations in mol/l)

K_{sp} = $CaCO_3$ solubility product

Ca, HCO_3, CO_{2aq} = calcium, bicarbonate and aqueous carbon dioxide concentration in mol/l respectively

T = temperature in °F

P = pressure in psig

I = ionic strength

Saturation Index for $Mg(OH)_2$

$$K_{spMgSO4} = IF(T < 60, -0.0001\times Ln(T) + 0.0006, -0.00009\times Ln(T) + 0.0005)\times 2$$
$$\times IF(T < 60, -0.0001\times Ln(T) + 0.0006, -0.00009\times Ln(T) + 0.0005)^2$$

Where:

T = temperature in °C

The derived $K_{spMgSO4}$ and IP values are used to determine the saturation index ($\log_{10}(IP/K_{sp})$)

Saturation Index for $CaSO_4$

$$SI_{gypsum} = \log(Ca \times SO_4) + 3.599 - 0.266\times10^{-3}T + 9.029\times10^{-6}T^2 - 5.586\times10^{-5}P$$
$$- 0.847I^{0.5} + 5.24\times10^{-2}I + 8.52\times10^{-2}I^{1.5} - 2.09\times10^{-3}TI^{0.5}$$

Where:

SI = $\log_{10}(IP/K_{sp})$

IP = Ionic Product = $[Ca^{2+}]$ $[SO_4^{2-}]$ (concentrations in mol/l)

K_{sp} = $CaSO_4$ solubility product

Ca, SO_4 = calcium and sulphate concentration in mol/l respectively

T = temperature in °F

P = pressure in psig

I = ionic strength

For streams above 90°C anhydrite becomes the stable form of calcium sulphate, the following equation for anhydrite formation applies:

$$SI_{anhydrite} = \log(Ca \times SO_4) + 2.884 + 9.327\times10^{-3}T + 0.188\times10^{-6}T^2 - 3.400\times10^{-5}P$$
$$-1.994I^{0.5} + 1.267I - 0.190I^{1.5} - 3.195\times10^{-3}TI^{0.5}$$

Where:

SI = $\log_{10}(IP/K_{sp})$
IP = Ionic Product = $[Ca^{2+}]$ $[SO_4^{2-}]$ (concentrations in mol/l)
K_{sp} = $CaSO_4$ solubility product
Ca, SO_4 = calcium and sulphate concentration in mol/l respectively
T = temperature in °F
P = pressure in psig
I = ionic strength

Saturation Index for $BaSO_4$

ASTM D4328-03 method

$$K_{spBaSO4} = \left(1.53\times10^{-13}T^2 - 5.41\times10^{-11}T + 1.03\times10^{-9}\right)I^2 + \left(5.36\times10^{-12}T^2 - 1.32\times10^{-10}T + 7.81\times10^{-9}\right)I$$
$$+1.19\times10^{-12}T^2 + 1.33\times10^{-10}T - 1.68\times10^{-9}$$

Where:

T = temperature in °C
I = ionic strength

The derived $K_{spBaSO4}$ and IP values are used to determine the saturation index ($\log_{10}(IP/K_{sp})$). This is applicable to streams that have a temperature of up to 95°C.

Oddo-Tomson method

$$SI = \log(Ba \times SO_4) + 10.147 - 4.946\times10^{-3}T + 11.650\times10^{-6}T^2 - 5.315\times10^{-5}P$$
$$-4.003I^{0.5} + 2.787I - 0.619I^{1.5} - 1.850\times10^{-3}TI^{0.5}$$

Where:

SI = $\log_{10}(IP/K_{sp})$
IP = Ionic Product = $[Ba^{2+}]$ $[SO_4^{2-}]$ (concentrations in mol/l)
K_{sp} = $BaSO_4$ solubility product
Ba, SO_4 = barium and sulphate concentration in mol/l respectively
T = temperature in °F
P = pressure in psig
I = ionic strength

Saturation Index for $SrSO_4$

ASTM D4328-03 method

$$\log K_{spSrSO4} = \frac{X}{R}$$

Where:

$$X = \frac{1}{T}, R = A + BX + CI^{\frac{1}{2}} + DI + EP^2 + FXP + GI^{\frac{1}{2}}P$$

T = temperature in °K

P = pressure in psig

I = Ionic Strength

$$A = 0.266948 \times 10^{-3}$$
$$B = -244.828 \times 10^{-3}$$
$$C = -0.191065 \times 10^{-3}$$
$$D = 53.543 \times 10^{-6}$$
$$E = -1.383 \times 10^{-12}$$
$$F = 1.103323 \times 10^{-6}$$
$$G = -0.509 \times 10^{-9}$$

The derived $K_{spSrSO4}$ and IP values are used to determine the saturation index ($\log_{10}(IP/K_{sp})$).

Oddo-Tomson method

$$SI = \log(Sr \times SO_4) + 6.090 + 2.237 \times 10^{-3} T + 5.739 \times 10^{-6} T^2 - 4.197 \times 10^{-5} P$$
$$- 2.082 I^{0.5} + 0.944 I - 8.650 \times 10^{-2} I^{1.5} - 1.873 \times 10^{-3} TI^{0.5}$$

Where:

SI = $\log_{10}(IP/K_{sp})$

IP = Ionic Product = $[Sr^{2+}]$ $[SO_4^{2-}]$ (concentrations in mol/l)

K_{sp} = $SrSO_4$ solubility product

Sr, SO_4 = strontium and sulphate concentration in mol/l respectively

T = temperature in °F

P = pressure in psig

I = ionic strength

Saturation Index for CaF_2

$$K_{spCaF_2T_n} = 7 \times 10^{-11} Ln(I) + 3 \times 10^{-10} \frac{-\Delta H}{R} \left(\frac{1}{T_n} - \frac{1}{298.15} \right)$$

Saturation Index for SiO_2

$$K_{spSiO2} = IF\left(\begin{array}{l} pH < 7, \left((2T + 75) \times \left(-9 \times 10^{-16}\, pH^2 - 0.125 pH + 1.875 \right) \right), \\ IF\left(AND\left(pH >= 7,\, pH <= 7.75 \right), \left((2T + 75) \times 1 \right), (2T + 75) \times \left(0.55 pH^2 - 8.56 pH + 34.413 \right) \right) \end{array}\right)$$

Where T and pH is the temperature in °C and pH of the stream respectively.